

Kondo temperature dependence of the Kondo splitting in a single-electron transistor

S. Amasha,¹ I. J. Gelfand,² M. A. Kastner,^{1,*} and A. Kogan^{1,†}

¹*Department of Physics, Massachusetts Institute of Technology, Cambridge, Massachusetts 02139, USA*

²*Division of Engineering and Applied Sciences, Harvard University, Cambridge, Massachusetts 02138, USA*

(Received 22 November 2004; revised manuscript received 8 March 2005; published 7 July 2005)

A Kondo peak in the differential conductance of a single-electron transistor is measured as a function of both the magnetic field and the Kondo temperature. We observe that the Kondo splitting decreases logarithmically with the Kondo temperature and that there exists a critical magnetic field B_C below which the Kondo peak does not split, in qualitative agreement with theory. However, we find that the magnitude of the prefactor of the logarithm is larger than predicted and is independent of B , in contradiction with theory. Our measurements also suggest that the value of B_C is smaller than predicted.

DOI: [10.1103/PhysRevB.72.045308](https://doi.org/10.1103/PhysRevB.72.045308)

PACS number(s): 73.23.Hk, 72.15.Qm, 75.20.Hr

The many-electron Kondo state is formed when conduction electrons screen a magnetic impurity. An important tool for studying the Kondo effect is the single-electron transistor (SET),¹⁻⁴ which consists of a confined droplet of electrons, called an artificial atom or a quantum dot, coupled by tunnel barriers to two conducting leads, called the source and the drain. When the quantum dot contains a net spin, the conduction electrons in the leads screen the spin on the dot and enhance the conductance of the SET. By using the gate electrodes that define the artificial atom to tune its parameters, Goldhaber-Gordon *et al.*⁵ have tested the predictions of renormalization group calculations and scaling theory and have shown that the equilibrium properties of the SET are quantitatively described by the Anderson Hamiltonian.

SETs also provide the unique possibility of exploring non-equilibrium Kondo phenomena by applying a dc voltage V_{ds} between the drain and the source. A sensitive test⁶⁻¹⁰ of the theories of nonequilibrium Kondo physics is the measurement of the splitting in a magnetic field B of the spin-1/2 Kondo peak in differential conductance as a function of V_{ds} . Calculations by Meir *et al.*⁶ predict that in a magnetic field the Kondo peaks occur at $eV_{ds} = \pm\Delta$, where $\Delta = |g|\mu_B B$ is the Zeeman energy for spin splitting and $\mu_B = 58 \mu\text{eV/T}$ is the Bohr magneton. We define Δ_K/e as half the separation in V_{ds} between the two peaks, so Meir *et al.* predict $\Delta_K = \Delta$. Early measurements by Cronenwett *et al.*⁴ agree with this prediction. However, calculations of spectral functions predict different features in the Kondo splitting. Costi⁷ predicts that the screening of the spin on the quantum dot by the conduction electrons should cause the Kondo peak to split only above a critical magnetic field B_C , which depends on the Kondo temperature T_K , the energy scale that describes the strength of the screening. Moore and Wen⁸ identify the field-induced splitting in their spectral function with the splitting in differential conductance and predict that the screening should cause $\Delta_K < \Delta$ at all fields and that Δ_K decreases logarithmically with increasing T_K . Recent observations by Kogan *et al.*¹¹ have confirmed the presence of the critical magnetic field B_C . However, the latter measurements, as well as those of Zumbühl *et al.*¹², show that $\Delta_K > \Delta$ at high fields, in disagreement with theory.

Here we extend the work of Kogan *et al.*¹¹ by reporting measurements of Δ_K as a function of the Kondo temperature

T_K , as well as B . These measurements exploit the property of SETs that T_K varies continuously with gate voltage, in contrast with conventional Kondo systems, for which T_K is determined by chemistry. We find $\Delta_K > \Delta$ for high fields at the lowest Kondo temperatures, as observed previously. We also observe that Δ_K decreases as $\ln(T_{K,0}/T_K)$ with increasing T_K , where $T_{K,0}$ is a constant. This logarithmic decrease in Δ_K with increasing T_K agrees qualitatively with theory. However, theory predicts that the decrease should be proportional to $|g|\mu_B B \ln(T_{K,0}/T_K)$, whereas we find the prefactor of the logarithm to be larger than predicted and independent of B . Our measurements also show that there is a critical magnetic field B_C for splitting the Kondo peak, as predicted. However, we find that the predicted values of B_C as a function of T_K appear to be too large.

The SET we study is fabricated from a heterostructure consisting of an undoped GaAs buffer, followed by a 15-nm layer of $\text{Al}_{0.3}\text{Ga}_{0.7}\text{As}$ δ -doped twice with a total of 10^{13} cm^{-2} of Si, and finally a 5-nm GaAs cap. The two-dimensional electron gas (2DEG) formed at the AlGaAs/GaAs interface has an electron density of $8.1 \times 10^{11} \text{ cm}^{-2}$ and a mobility of $10^5 \text{ cm}^2/\text{V s}$ at 4.2 K. Although the density of the 2DEG is high, magnetotransport measurements show that only a single subband is occupied. Electron-beam lithography is used to define the gate electrode pattern shown in the inset of Fig. 2(b). Applying a negative voltage to these electrodes depletes the 2DEG underneath them and forms an artificial atom of about 50 electrons isolated by two tunnel barriers from the remaining 2DEG regions, the source and drain leads. The electrochemical potential of the dot, as well as the coupling between the dot and the leads, can be tuned by changing the voltages on the electrodes. The voltage on the gate electrode g is denoted V_g . The SET is measured in a 75 μW Oxford Instruments dilution refrigerator with an 8 T magnet and a lowest electron temperature of about 100 mK. To minimize orbital effects we align the 2DEG parallel to the magnetic field to within a few degrees. We measure the differential conductance dI/dV_{ds} utilizing standard lock-in techniques.

To compare Δ_K to Δ we need an accurate measurement of the Zeeman splitting, and hence $|g|$, in our SET. Such measurements were reported for this SET in Ref. 11 and the

results are summarized here. We measured the Zeeman splitting in this SET using the traditional method of electron addition spectroscopy and the more precise method of inelastic spin-flip cotunneling. These measurements showed that Δ was linear with field up to 7.8 T and the slope was given by $|g|=0.16$. We also used inelastic cotunneling to measure the Zeeman splitting in an identical device in a different dilution refrigerator with a lower electron temperature and a larger magnet. In this setup, the device was aligned parallel to the magnetic field to better than 0.5° . Measurements of this sample showed that Δ was linear with field up to a magnetic field of 14 T and that $|g|$ was consistent with the value measured in the other device. We attribute the small g factor to the penetration of the electron wave function into the Al-GaAs. We believe the large electric fields produced by the relatively high electron density enhances this effect. Measurements of the Kondo splitting in a magnetic field in both devices showed that Δ_K increased linearly with the field with a slope given by $|g|$; however in both devices $\Delta_K > \Delta$ by about $10 \mu\text{eV}$.

We observe the Kondo effect by tuning the gate voltages so that the artificial atom is strongly coupled to the leads. Figure 1(a) shows an example of a plot of dI/dV_{ds} as a function of V_{ds} and V_g for this device. Enhancements in the conductance at $V_{ds}=0$ in the middle of every second Coulomb blockade valley are clearly visible. We infer that the valleys with Kondo peaks are those with an odd number of electrons. A sharp peak in dI/dV_{ds} at $V_{ds}=0$, for V_g between the Coulomb charging peaks, where resonant tunneling is prohibited by energy and charge conservation, is the hallmark of the Kondo effect. The gate lithography makes this device very small, resulting in typical excited state energies on the order $300\text{--}400 \mu\text{eV}$. The large excited state energies can be seen explicitly in Fig. 1(a) by the location of the orbital inelastic cotunneling thresholds in the even valleys. It has been demonstrated in both AlGaAs/GaAs and carbon nanotube SETs that a perpendicular magnetic field^{12–15} or gate voltage^{16–18} can reduce the energy of the excited state and lead to higher spin Kondo states. The large excitation energy in our device makes this transition unlikely, especially since our magnetic field is parallel to the 2DEG, and we see no evidence for this transition in our data. For the remainder of this paper we focus on studying spin-1/2 Kondo physics.

An example of a peak at $B=0$ T is shown in Fig. 1(c). Applying a magnetic field causes the Kondo peak to split into two peaks above and below $V_{ds}=0$. This is shown in Fig. 1(b), while Fig. 1(c) shows dI/dV_{ds} vs V_{ds} at various magnetic fields. To study the splitting of a Kondo peak in dI/dV_{ds} as a function of T_K , we take advantage of the fact that T_K varies across a Coulomb valley. The dependence of T_K on the energy ϵ_0 of an unpaired electron in the artificial atom referenced to the Fermi level is predicted to be^{5,19}

$$T_K = \frac{\sqrt{\Gamma U}}{2k_B} \exp[\pi\epsilon_0(\epsilon_0 + U)/\Gamma U]. \quad (1)$$

Here Γ is the full width at half maximum of the Coulomb charging peaks and U is the charging energy necessary to add an electron to the artificial atom. Goldhaber-Gordon *et*

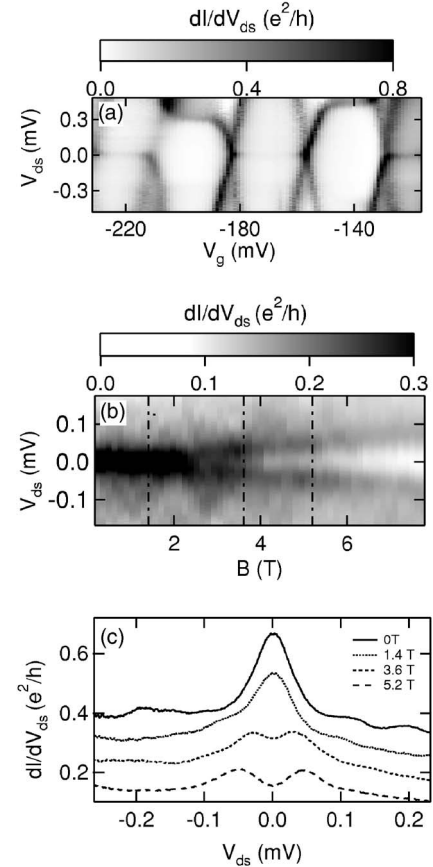


FIG. 1. (a) Examples of Coulomb blockade diamonds when the artificial atom is strongly coupled to the leads. The Kondo effect shows up as sharp resonances near $V_{ds}=0$ in the odd valleys. The inelastic cotunneling thresholds in the even valleys indicate the energies of the excited states. These data are at different electrode voltages and during a different cool down of the device from those in the rest of the paper. (b) The evolution of a Kondo peak as a function of magnetic field. Note that the splitting does not begin until $B=2.4$ T. (c) dI/dV_{ds} vs V_{ds} for $B=0$ T and for other values of B marked by the dash-dot lines in (b). For $B < 2.4$ T there is only one Kondo peak; above the threshold it splits. The traces have been offset by $0.08e^2/h$ for clarity.

*al.*⁵ have shown that their measurements of T_K are fit well by this equation. Expressing T_K in terms of its value in the middle of the Coulomb valley

$$T_K = T_{K,0} \exp[\pi(\Delta\epsilon)^2/\Gamma U]. \quad (2)$$

In this equation, $T_{K,0}$ is the Kondo temperature in the middle of the Coulomb valley, and $\Delta\epsilon$ is the difference in the energy from its value in the middle of the valley. $\Delta\epsilon$ is related to the gate voltage by $\Delta\epsilon = \alpha_g e(V_g - V_{g,0})$ where α_g is the ratio of the gate capacitance to the total capacitance and $V_{g,0}$ is the value of V_g in the middle of the valley. We can thus rewrite the argument of the exponential in Eq. (2) as $\chi(V_g - V_{g,0})^2$, where $\chi = \pi\alpha_g^2 e^2/\Gamma U$. The Kondo temperature is a minimum in the middle of the Coulomb valley and increases exponentially close to the Coulomb blockade peaks. Thus, by varying V_g , we can study the variation in Δ_K as a

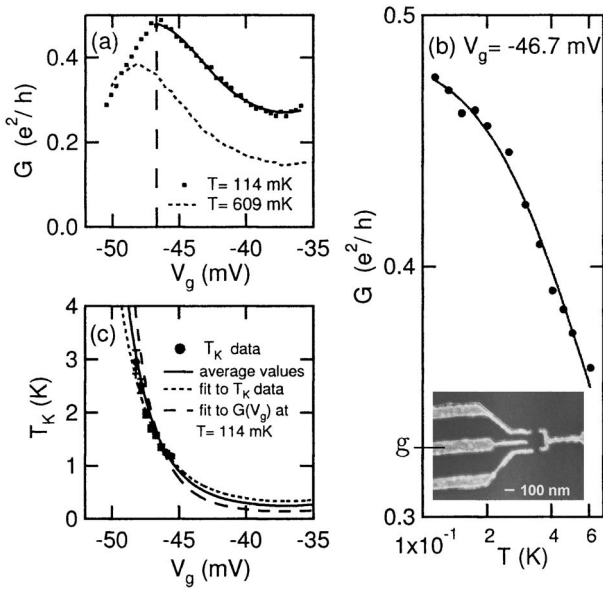


FIG. 2. (a) dI/dV_{ds} vs V_g at $V_{ds}=0$ (denoted G) for a Coulomb charging peak and half a Coulomb valley at two different temperatures. The solid line is a fit to Eqs. (2) and (3) and is discussed in the text. (b) G as a function of temperature for the value of V_g marked by the dashed vertical line in (a). Fitting these data to Eq. (3) gives $T_K=1.57\pm 0.05$ K. The inset shows an electron micrograph of a SET similar to the one we have studied. (c) The dots show T_K determined as in (b) as a function of V_g . The dotted line is the result of fitting these data to Eq. (2). The dashed line shows T_K as a function of V_g using the results of the fit shown in (a). The solid black line shows T_K for the parameter values $\chi=0.020$ (mV) $^{-2}$ and $T_{K,0}=250$ mK.

function of T_K . If the Kondo temperature gives a logarithmic correction to the splitting as predicted,⁸ then we expect Δ_K to vary quadratically in gate voltage.

To make quantitative comparisons with theory we need to determine T_K for a range of V_g . To determine T_K at a fixed gate voltage we follow Goldhaber-Gordon *et al.*⁵ and measure the differential conductance at $V_{ds}=0$ (denoted G) as a function of temperature. We then fit these data to an empirical form that gives a good approximation to numerical renormalization group results²⁰ to obtain the Kondo temperature T_K . The empirical form is given by

$$G(T) = G_0[1 + (2^{1/s} - 1)(T/T_K)^2]^{-s}, \quad (3)$$

where $s=0.22$ for the spin-1/2 Kondo effect. This fit is accurate only if we have data for temperatures as low as $T \sim 0.1T_K$. The lowest temperature we can achieve is about 100 mK, so we can reliably measure Kondo temperatures larger than approximately 1 K. The Kondo temperature in the middle of the Coulomb blockade valley is significantly lower than this, so we cannot measure it directly. However, we can measure T_K near the Coulomb blockade peaks where the Kondo temperature is much higher. Fitting the latter data for T_K as a function of V_g to Eq. (2) we can determine $T_{K,0}$ and χ .

Figure 2 illustrates this procedure. Figure 2(a) shows a

Coulomb charging peak and half the Coulomb valley at two different temperatures. As the temperature is raised, the suppression of the Kondo effect removes the energy renormalization, causing the peak to move toward the bare resonance.^{5,21} We measure G as a function of temperature at several values of V_g , one of which is shown in Fig. 2(b), and fit these data to the empirical form given by Eq. (3) to determine T_K . Finally, the data points in Fig. 2(c) show T_K as a function of V_g for the range in which it can be determined with confidence. Fitting these data to Eq. (2), shown by the dotted line in Fig. 2(c), we find $T_{K,0}=340$ mK and $\chi=0.016$ (mV) $^{-2}$.

Another way of determining T_K is to take advantage of the fact that G_0 is independent of the gate voltage between the bare Coulomb resonances⁵. Combining Eq. (2) and (3) gives an equation for $G(V_g)$ at a fixed temperature with fit parameters χ , $T_{K,0}$, and G_0 . We use this equation to fit the $G(V_g)$ data at $T=114$ mK, shown in Fig. 2(a). The fit is shown as the solid line through the data and gives $T_{K,0}=145$ mK and $\chi=0.026$ (mV) $^{-2}$. A plot of T_K vs V_g for these fit parameters is shown by the dashed line in Fig. 2(c). From these two methods, we arrive at the values $\chi=0.020\pm 0.006$ (mV) $^{-2}$ and $T_{K,0}=250\pm 100$ mK. A plot of T_K vs V_g determined from these parameters is shown as the solid line in Fig. 2(c). We can use our value of χ to estimate Γ . From nearby Coulomb charging diamonds, we estimate $U=1.2$ mV and $\alpha_g=0.05$. Combining this with our value of $\chi=0.020$ (mV) $^{-2}$ we find that $\Gamma \approx 330$ μ eV. Our values are similar to those obtained by Goldhaber-Gordon *et al.*,⁵ who found $U=1.9\pm 0.05$ meV, $\alpha_g=0.069\pm 0.0015$, and $\Gamma=280\pm 10$ μ eV, and are consistent with having a somewhat larger artificial atom with stronger coupling to the leads. As expected for this stronger coupling, $T_{K,0}$ in our SET is larger than that of Goldhaber-Gordon *et al.*⁵

To study the dependence of Δ_K on T_K we measure dI/dV_{ds} as a function of V_{ds} and V_g at various magnetic fields. An example of such a measurement is shown in Fig. 3(a), while Fig. 3(c) shows dI/dV_{ds} vs V_{ds} traces at the values of V_g marked in Fig. 3(a). We determine the position of a peak by fitting the data points in the neighborhood of the peak to a parabola. The center of the parabola determines the peak position. At a given V_g , Δ_K is half the separation between the positions of the positive and negative peaks. The values of Δ_K as a function of V_g are shown in Fig. 3(b). These data are fit very well by a parabola, which is shown in the figure. As discussed above, a parabola is what one would expect from a correction to Δ_K that is logarithmic in the Kondo temperature.

One important feature of these data is that for $B > 4$ T, the maxima of the Δ_K vs V_g curves lie above $\Delta = |g|\mu_B B$, where the value of Δ is determined precisely using inelastic cotunneling.¹¹ By fitting $\Delta_K(V_g)$ to a parabola, we extract the maximum value of Δ_K , which is plotted as a function of magnetic field in Fig. 4(a). The solid line shows the value of Δ from cotunneling measurements. These data show that for large magnetic fields, $\Delta_K > \Delta$ by about 10 μ eV, as observed previously.^{11,12}

Another important feature of these data is the curvature of the parabolas, which is plotted versus B in Fig. 4(b). Moore

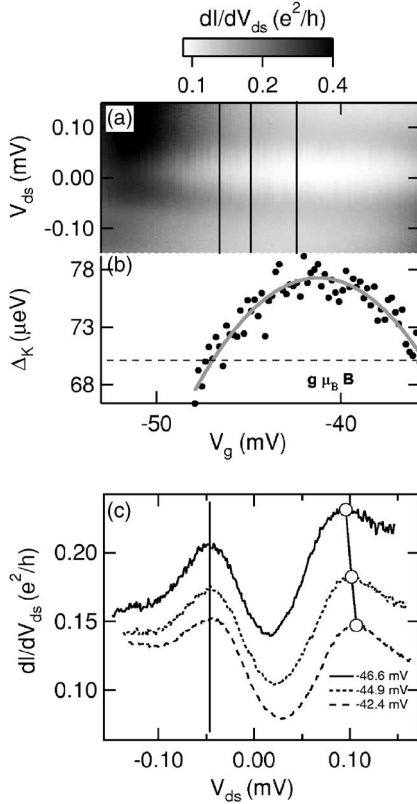


FIG. 3. (a) A Kondo feature in a 7.5-T magnetic field. The Kondo peak at zero bias has clearly split into two peaks. One Coulomb charging peak is visible at $V_g = -52$ mV; the other peak is not visible. (b) Δ_K as a function of V_g . The splitting is a maximum in the center of the valley, where the Kondo temperature is lowest. The gray line shows the result of fitting the data to a parabola. The dashed horizontal line indicates the Zeeman energy $|g|\mu_B B$. Note that the splitting in the middle of the valley exceeds $|g|\mu_B B$. (c) dI/dV_{ds} vs V_{ds} for the values of V_g marked by the lines in (a). The traces have been shifted horizontally so that the peaks at negative V_{ds} are aligned. The circles mark the positions of the peaks at positive V_{ds} , showing that the splitting between the peaks changes with gate voltage.

and Wen⁸ predict that for $1 < \Delta/k_B T_K < 100$, $\Delta_K/\Delta = b \ln(\Delta/k_B T_K) + \text{constant}$, where b is a constant of proportionality and is approximately 0.06. From Eq. (2), T_K varies exponentially with the gate voltage so that at a fixed magnetic field the prediction is $\Delta_K = \Delta_{K,0} - b(|g|\mu_B B)\chi(V_g - V_{g,0})^2$, where $\Delta_{K,0}$ gives the field splitting at the center of the valley. This is the equation of a parabola in V_g whose curvature becomes more negative with increasing magnetic field. This prediction is plotted in Fig. 4(b) for $\chi = 0.020$ (mV)⁻² and clearly does not agree with the data. The magnitude of the curvature is much larger than predicted by theory, except at the highest fields, and does not grow with increasing magnetic field. The constant curvature of the data indicates that the correction to the Kondo splitting is given by $c \ln(T_{K,0}/T_K)$, where c is a constant; by comparing to the data we find $c = 12$ μeV .

We can also use these data to test predictions about the threshold field B_C necessary to split the Kondo peak. The existence of a threshold field is illustrated in Fig. 1(b). The

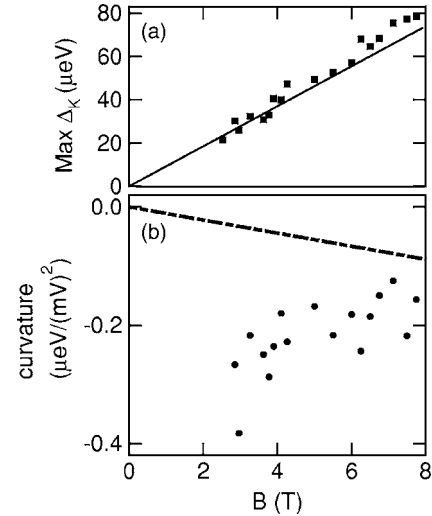


FIG. 4. (a) Splitting of the Kondo peak in the center of the Coulomb valley as a function of the magnetic field. The solid line shows $\Delta = |g|\mu_B B$ for $|g| = 0.16$ determined by inelastic cotunneling. Above ~ 4 T we find that $\Delta_K > |g|\mu_B B$. Below $B = 2.4$ T, no splitting is observed. (b) The curvature of Δ_K vs V_g parabolas like that in Fig. 3(b). The prediction of Moore and Wen (Ref. 8) (dashed line) is that the curvature should decrease with field.

peak does not start to split until B is greater than about 2.4 T. Figure 5(a) shows this threshold in more detail: at $B = 2.0$ T the peak has not yet split, but by 2.4 T, the splitting is clearly evident. We can also extract information about B_C from data like those in Fig. 5. For a given magnetic field there is some Kondo temperature $T_{K,C}$ for which this field is the critical field. For T_K below $T_{K,C}$, the Kondo peak is split and for T_K greater than $T_{K,C}$ the peak is not split. This is illustrated by the data in Figs. 5(b) and 5(c), which shows some individual traces from Fig. 5(b). In the middle of the valley, where the Kondo temperature is lowest, the peak is clearly split. This splitting disappears toward the Coulomb charging peak where the Kondo temperature is higher. Because of the background from the Coulomb charging peak, it is difficult to reliably locate $T_{K,C}$. Instead, we identify a range of Kondo temperatures over which we are confident that the peak is split: this puts a lower bound on $T_{K,C}$.

To extract this bound, we locate the most negative gate voltage at which we still confidently observe the Kondo splitting. For the data in Figs. 5(b) and 5(c), this is at $V_g = -49.9$ mV. To convert this to a Kondo temperature we use Eq. (2). To find the center of the valley $V_{g,0}$, we use the location of the maximum of the fit of $\Delta_K(V_g)$ to a parabola. We take into account the uncertainty in the determination of $V_{g,0}$ to make the most conservative estimate of the lower bound. Knowing $V_{g,0}$ we can convert V_g into a Kondo temperature using Eq. (2). The lower bounds on $T_{K,C}$ found in this way using $\chi = 0.020$ (mV)⁻² and $T_{K,0} = 250$ mK are shown as data points in Fig. 5(d). The error bars show the Kondo temperatures extracted using the other two sets of χ and $T_{K,0}$ shown in Fig. 2(c) and taking into account errors on these values. At Kondo temperatures below these data points, the Kondo peak is split.

We can use our data to check predictions about $T_{K,C}$. Costi⁷ predicts that $B_C = 0.5T_{\text{HWHM}}$, where T_{HWHM} is the half

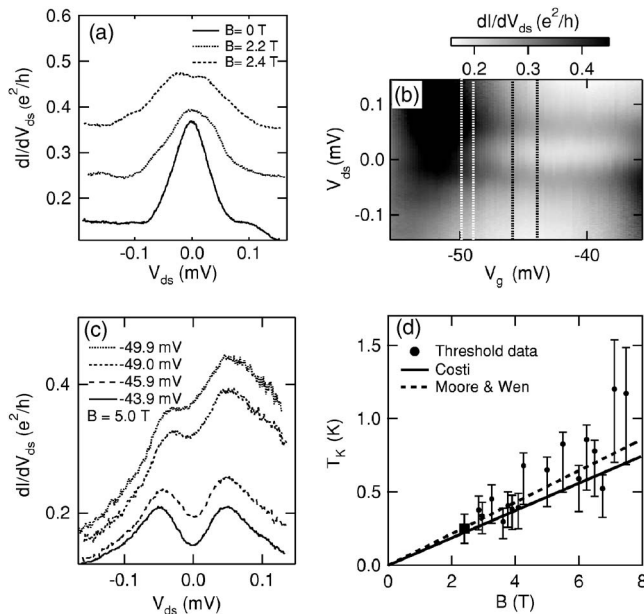


FIG. 5. (a) Drain-source sweeps in the middle of a Kondo valley at different magnetic fields. The onset of splitting is clear at $B = 2.4$ T but not visible at 2.2 T. The curves have been offset by $0.11e^2/h$ for clarity. (b) A Kondo valley with a 5-T field applied. The lines indicate the positions of the dI/dV_{ds} vs V_{ds} traces shown in (c). (c) dI/dV_{ds} vs V_{ds} at various gate voltages. In the center of the valley where T_K is a minimum, the splitting is clear and symmetric. Closer to the charging peak the Kondo temperature is higher and the splitting is less pronounced but still visible. (d) The dots mark the maximum T_K at which splitting is observed as a function of field. These data are extracted from data like those in (b) and (c) by measuring the gate voltage at which the splitting is barely visible. The conversion of this gate voltage to a Kondo temperature is explained in the text. The square data point at $B=2.4$ T marks the measurement of B_C from the data in (a). Predictions for B_C of Costi (Ref. 7) (solid line) and Moore and Wen (Ref. 8) (dashed line) are shown.

width at half maximum of the Kondo resonance in the spectral function at $T=0$ and is related^{7,22} to T_K by $T_K = 0.433T_{\text{HWHM}}$. This prediction is shown as the solid line in

Fig. 5(d): Costi predicts that below this line the Kondo peak should be split and above it the Kondo peak should not be split. However, this line lies below the lower bound set by some of our data points suggesting that at a given T_K , B_C is smaller than predicted by theory. The dotted line in Fig. 5(d) is based on the work of Moore and Wen, who predict⁸ the width and splitting of the spin-up component of the spectral function as a function of B/T_K . To model the Kondo peak arising from this spectral function we sum two lorentzians²³ with the width and splitting given by the predictions of Moore and Wen. We find that the splitting appears at $B_C = T_K$. This prediction is plotted as a dashed line in Fig. 5(d) and lies below several data points at higher magnetic fields.

The observation that $\Delta_K > \Delta$ by Kogan *et al.*¹¹ and Zumbühl *et al.*¹² demonstrates that we do not yet have a full theoretical understanding of the nonequilibrium Kondo effect. Our measurements of the Kondo temperature dependence of Δ_K reinforce this conclusion. While theory qualitatively describes the behavior of Δ_K with T_K , it does not provide an accurate quantitative description. We find that Δ_K decreases logarithmically with increasing T_K , but the prefactor of the logarithm is larger than expected at low fields and is independent of B . There is clear evidence of a critical field B_C for the splitting of the Kondo peak, again in qualitative agreement with theory. However, our data suggest that B_C is smaller than predicted by theory. Our results provide additional challenges to the theory of the nonequilibrium Kondo effect.

We thank D. Goldhaber-Gordon and D. Mahalu for designing and fabricating the SET devices used in this work and H. Shtrikman for growing the GaAs/AlGaAs heterostructures. We are grateful to J. Moore, T. Costi, L. Levitov, X.-G. Wen, W. Hofstetter, C. Marcus, D. Zumbühl, and J. Folk for discussions, and to C. Cross, G. Granger, and K. MacLean for experimental help. This work was supported by the US Army Research Office under Contract No. DAAD19-01-1-0637, by the National Science Foundation under Grant No. DMR-0353209, and in part by the NSEC Program of the National Science Foundation under Award No. DMR-0117795, and the MRSEC Program of the National Science Foundation under Award No. DMR 02-13282.

*Electronic address: mkastner@mit.edu

[†]Present address: Department of Physics, University of Cincinnati, Cincinnati, OH 45221-0011.

¹L. I. Glazman and M. E. Raikh, JETP Lett. **47**, 452 (1988).
²T. K. Ng and P. A. Lee, Phys. Rev. Lett. **61**, 1768 (1988).
³D. Goldhaber-Gordon, H. Shtrikman, D. Mahalu, D. Abush-Magder, U. Meirav, and M. A. Kastner, Nature (London) **391**, 156 (1998).
⁴S. M. Cronenwett, T. H. Oosterkamp, and L. P. Kouwenhoven, Science **281**, 540 (1998).
⁵D. Goldhaber-Gordon, J. Göres, M. A. Kastner, H. Shtrikman, D. Mahalu, and U. Meirav, Phys. Rev. Lett. **81**, 5225 (1998).
⁶Y. Meir, N. S. Wingreen, and P. A. Lee, Phys. Rev. Lett. **70**, 2601

(1993).

⁷T. A. Costi, Phys. Rev. Lett. **85**, 1504 (2000).

⁸J. E. Moore and X.-G. Wen, Phys. Rev. Lett. **85**, 1722 (2000).

⁹A. Rosch, J. Paaske, J. Kroha, and P. Wölfle, Phys. Rev. Lett. **90**, 076804 (2003).

¹⁰A. Rosch, T. A. Costi, J. Paaske, and P. Wölfle, Phys. Rev. B **68**, 014430 (2003).

¹¹A. Kogan, S. Amasha, D. Goldhaber-Gordon, G. Granger, M. A. Kastner, and H. Shtrikman, Phys. Rev. Lett. **93**, 166602 (2004).

¹²D. M. Zumbühl, C. M. Marcus, M. P. Hanson, and A. C. Gossard, Phys. Rev. Lett. **93**, 256801 (2004).

¹³S. Sasaki, S. D. Franceschi, J. M. Elzerman, W. G. van der Wiel, M. Eto, S. Tarucha, and L. P. Kouwenhoven, Nature (London)

- 405**, 764 (2000).
- ¹⁴W. G. van der Wiel, S. De Franceschi, J. M. Elzerman, S. Tarucha, L. P. Kouwenhoven, J. Motohisa, F. Nakajima, and T. Fukui, *Phys. Rev. Lett.* **88**, 126803 (2002).
- ¹⁵J. Nygard, D. H. Cobden, and P. Lindelof, *Nature (London)* **408**, 342 (2000).
- ¹⁶A. Kogan, G. Granger, M. A. Kastner, D. Goldhaber-Gordon, and H. Shtrikman, *Phys. Rev. B* **67**, 113309 (2003).
- ¹⁷J. Kyriakidis, M. Pioro-Ladriere, M. Ciorga, A. S. Sachrajda, and P. Hawrylak, *Phys. Rev. B* **66**, 035320 (2002).
- ¹⁸A. Fuhrer, T. Ihn, K. Ensslin, W. Wegscheider, and M. Bichler, *Phys. Rev. Lett.* **91**, 206802 (2003).
- ¹⁹F. D. M. Haldane, *Phys. Rev. Lett.* **40**, 416 (1978).
- ²⁰T. A. Costi, A. C. Hewson, and V. Zlatić, *J. Phys.: Condens. Matter* **6**, 2519 (1994).
- ²¹N. S. Wingreen and Y. Meir, *Phys. Rev. B* **49**, 11040 (1994).
- ²²T. A. Costi (private communication).
- ²³J. E. Moore (private communication).